

RHIC Program, Its Origin and Early Results

Wit Busza, John W. Harris, and Shoji Nagamiya

Abstract At the Brookhaven National Laboratory, experimental efforts with heavy-ion accelerators started at the AGS synchrotron in 1984 and then at the Relativistic Heavy Ion Collider (RHIC) in 1991. This chapter describes how several scientific collaborations were established and how features of the quark-gluon plasma were revealed from the four RHIC experiments during the first five years of RHIC operation.

1 RHIC Origins

By the late 1970s an exponentially growing community was born, interested in studying ultra-relativistic heavy-ion collisions.¹ It was a merger of particle physicists interested in the mechanism of multiparticle production in high energy hadronic collisions and nuclear physicists interested in investigating the nuclear equation of state and what happens when nuclear matter is compressed. These interests were further heightened by the discovery of quarks and gluons, asymptotic freedom, the existence of neutron stars, and the development of the theory of Quantum Chromodynamics (QCD). This led to the realization that, in essence, the two groups were interested in the same physics; the condensed matter of QCD at ultra-high energy density and temperature. Furthermore, it was realized that this field had some fascinating and important questions that needed to be answered. Is the vacuum around us unique? Do different forms of nuclear matter exist? Does a phase of QCD matter

Wit Busza
MIT; e-mail: busza@mit.edu

John W. Harris
Yale University; e-mail: john.harris@yale.edu

Shoji Nagamiya
KEK; e-mail: nagamiya@post.kek.jp

¹ See previous chapter in this book by W. Busza and W. Zajc

exist in which quarks and gluons are free? Does there exist a phase in which chiral symmetry is restored? What does the complete phase diagram of QCD matter look like? Can any of these phases be created and studied in the laboratory? An added interest in these questions was the realization that in the early universe, about 10 microseconds after the big bang, the hadronic part of the entire universe was thought to be in a gas-like state of free and noninteracting quarks and gluons, a state to which the name “quark-gluon plasma” was given, or “QGP”² for short.

Interest in these questions led to numerous workshops and conferences. It also stimulated discussions on whether current accelerators could be used to address some of these issues and whether new accelerators or colliders needed to be constructed. After a landmark recommendation³ in 1983 and the unanticipated availability of an unfinished ISABELLE/CBA collider complex at Brookhaven National Laboratory (BNL) [1], there was considerable interest in a possible relativistic heavy-ion collider at BNL. A special round-table discussion by a distinguished international panel of nuclear and high-energy physicists was held at the 1983 Quark Matter Conference at BNL to discuss the future of relativistic heavy-ion physics, and led to the RHIC experimental program followed by an LHC heavy-ion program at CERN [2].

An obvious concern, which ultimately could only be answered experimentally, was whether any existing accelerator, or the future RHIC, could produce a state that has sufficiently high energy density and lasts for a sufficiently long time to create an interesting new kind of QCD matter, such as the QGP. In the 1970s/1980s, based on the assumption that a QGP was a gas of noninteracting quarks and gluons, knowledge of the masses and sizes of hadrons, and the Hagedorn temperature [3] (where there is a very rapid increase in the number of hadron levels with mass), it was believed that for the creation of a QGP one needed an energy density of the order of or greater than 1 GeV/fm^3 .

The community was full of optimism that 1 GeV/fm^3 would be achieved at RHIC, and further encouraged by extrapolations of Fermilab p-A data [4], which showed that high-energy protons that traverse large nuclei lose about 2 units of rapidity. Thus, suggesting that in head-on heavy-ion collisions about 85% of the incident energy will be deposited in the collision. Experiments confirmed these estimates [5]. At the AGS energy of 14 A-GeV for a projectile impinging on a target at rest, it was observed that the two nuclei stop each other in their center of mass, while on the other hand they penetrate through each other at the higher SPS energies of 200 A-GeV. Thus, it was expected that at the much higher energies of RHIC, the colliding nuclei would penetrate each other completely and create a hot baryon-free region, as schematically illustrated in Fig. 1. Although expectations were that at RHIC

² Prior to RHIC, the community had adopted the term “QGP” to describe any system that is best described in terms of quark and gluon degrees of freedom. There was already some caution from theory that the QGP could not be an ideal gas of deconfined, weakly interacting quarks and gluons. As soon as the RHIC results exhibited strong collectivity, it was realized that the QGP had to be strongly interacting.

³ The US Nuclear Science Advisory Committee identified the scientific opportunities of a relativistic heavy-ion collider and recommended it as the next major construction project for nuclear science in the US. See https://science.osti.gov/-/media/np/nsac/pdf/docs/lrp_1983.pdf

energies the all-important energy density in the hot region would exceed 1 GeV/fm^3 , experimental confirmation was necessary. In short, it needed the construction of RHIC and its detectors!

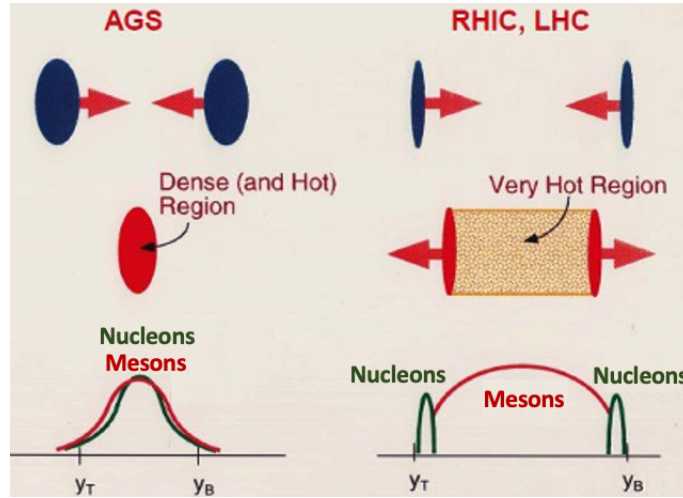


Fig. 1 Schematic diagram of a collision of two nuclei at the AGS (left column), and at RHIC and the LHC (right column), as described in the text. At bottom are shown the corresponding rapidity (y) distributions after the collision.

Given the above interest and expectations, a much-publicized workshop was held at BNL on July 4, 1990, to initiate discussion of the RHIC experiments. It was a particularly important workshop in that the BNL RHIC project had just been included in the President's proposed FY 1991 budget as a new construction item, and a call for letters of intent (LoIs) for RHIC experiments had been issued at the BNL Users meeting in May 1990. A workshop was held in July 1990 to form collaborations and prepare LoIs. Eight LoIs⁴ to study A-A collisions at RHIC were submitted to the BNL High Energy Nuclear Physics Program Advisory Committee in November 1990. Guided by almost a year of discussions, including a community-wide meeting in April 1991, four proposals for experiments were submitted in 1991: STAR to measure charged particles over 4π ; OASIS to measure identified hadrons, photons, and e^+e^- pairs; Dimuon to measure $\mu^+\mu^-$ pairs; and TALES/SPARHC to measure e^+e^- pairs. The proposed detectors, among them, covered the full phase space of all

⁴ RLOI-2, TALES/SPARHC: Two-Arm Electron/Photon/Hadron Spectrometer; RLOI-3, Search for a Quark-Gluon Plasma and Other New Phenomena with a 4π Tracking TPC Magnetic Spectrometer at RHIC; RLOI-4, A Dimuon Spectrometer for RHIC Measurements of Muon Pairs, Vector Mesons, and Photons; RLOI-5, STAR: An Experiment on Particle and Jet Production at Midrapidity; RLOI-6, MARS (later became PHOBOS): A Modular Array for RHIC Spectra; RLOI-7, OASIS: Open Axially Symmetric Ion Spectrometer; RLOI-8, (later became BRAHMS) Forward Angle Hadron Spectrometer Experiment at RHIC; RLOI-9, High p_T Photons, Charged Particles and Jets at RHIC.

of the produced particles and would be more than adequate to investigate heavy-ion collisions at RHIC. However, obviously all were not within the budget of the RHIC program, and thus decisions had to be made on what to build. These proposals were sent to BNL and a meeting of the BNL High Energy Nuclear Physics Program Advisory Committee was held in September 1991 to consider the proposals.

Management decided that there would be two large general-purpose detectors, but with different physics strengths. The STAR experiment was approved, while the three others were advised to merge and then formed the PHENIX experiment in 1992. STAR, PHENIX and a smaller experiment PHOBOS were given final approval at the BNL High Energy Nuclear Physics Program Advisory Committee meeting in September 1992.

The funding from the U.S. Department of Energy was set at \$30M for each of the large detectors, and additional resources, if needed, would have to be arranged by the individual experimental groups. BRAHMS, a two-arm hadron spectrometer, was approved later as one of the small detectors. The RHIC complex with its four experiments is shown in Fig. 2 and described in [6].

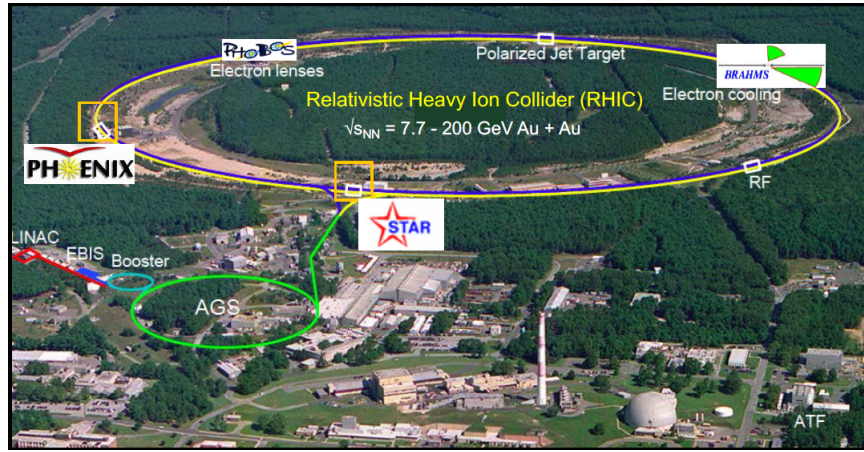


Fig. 2 The RHIC Complex and its four detector experiments. See [6] for reference and details.

2 The STAR Experiment at RHIC

2.1 Conception of the STAR Experiment at RHIC

The concept and design of the STAR experiment were created after an almost-year-long series of weekly meetings and discussions. A series of RHIC Planning Meetings

was held at LBL (October '89 - July '90) where theorists and experimentalists were invited to discuss potential defining measurements at a future Relativistic Heavy Ion Collider (RHIC). In total 24 presentations were made on various topics on detector technologies and relativistic heavy-ion theory over that time frame, with the goal of deciding on the specifications of an experiment that would address important questions of the field.

In addition, it was recognized that a new large-scale RHIC experiment would be novel to nuclear physics and *new detector techniques* would need to be considered. Those included time projection chambers (TPCs), ring-imaging Cherenkov (RICH) detectors, photon detectors, charge-coupled devices (CCDs), smart calorimeters, scintillating fibers, and more. Furthermore, *data acquisition* systems would be encumbered by large event sizes, and the continued development of high-density fast integrated electronics would further exacerbate the problem. Thus, rapid online data reduction would be necessary, but advances in large-scale fast data storage devices and media would still be needed. Together, several complex detector systems would be integrated into one experiment.

There were *sociological and operational factors* that had to be considered. Although perhaps not new to high-energy physicists, this was new to our community. A large research collaboration would need to form in order to carry out all aspects of such an experiment - including its design, integration of detector systems, construction, operation, and physics. This would require better communication, planning, organization, and management. Lessons would be learned, and advice from the high-energy community was very welcome. The long-term aspects of such an experiment also required a new look at traditional hiring practices in experimental nuclear physics. We were getting prepared for the challenge, but was nuclear physics in general prepared for RHIC?

2.2 STAR Physics and Experiment

The physics goals and a conceptual design were starting to converge by January 1990. The primary focus for RHIC and the STAR physics program in general was the study of QCD at high energy density and temperature. The STAR approach was to have a large acceptance detector that would maximize the information recorded per collision. In the absence of definitive signatures for the QGP, the high track multiplicities should allow the extraction of global observables such as centrality, temperature, reaction plane, and the mean transverse energy $\langle E_T \rangle$.

In a search for possible QGP signatures, the STAR experiment was initially focused on the measurement and correlation of as many observables as possible on an event-by-event basis. The physics goals could be divided into i) the study of soft (non-perturbative) physics processes, i.e., low p_T hadron production, and ii) the study of hard (perturbative) QCD processes, i.e. jet, mini-jet, and high- p_T particle production. The physics program also included the measurement of the spin structure

function of the proton, and the study of photon and pomeron interactions from the large electromagnetic fields created by the passing heavy ions at RHIC.

To meet these goals, STAR was designed to have large uniform acceptance, good momentum and two-track resolution, and particle identification capabilities to facilitate measurement of many observables. The STAR detector is shown in Fig. 3 and described in [7]. Examples of such measurements included particle spectra, flavor composition, particle interferometry, as well as density fluctuations of energy, entropy, and multiplicity in azimuth and pseudorapidity. The remnants of hard-scattered partons were used as a penetrating probe of the QGP, and expected to provide important new information on the nucleon structure function and parton shadowing in nuclei.

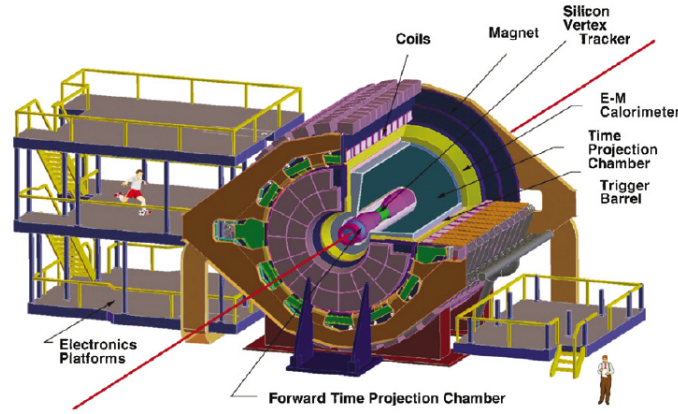


Fig. 3 The STAR Detector and its sub-detector systems as labeled. See [7] and references therein for details.

An initial physics goal of STAR was to measure the relative concentration of strange and non-strange quarks on an event-ensemble basis, as well as strange and anti-strange baryons over a wide rapidity interval about mid-rapidity. Enhancements in strange antibaryon content were predicted in QGP formation, with multi-strange baryons expected to be even more sensitive to the existence of the QGP. [8]

Measurements of strange and anti-strange baryons required detection of secondary decay vertices of particles within a distance $c\tau \sim 2\text{-}8$ cm from the primary collision vertex. The tracking capabilities of a time projection chamber in STAR provided an azimuthally complete acceptance over a large rapidity interval. These qualities were essential for measuring the production of strangeness and open charm in collisions at RHIC in the search for the QGP. The STAR experiment, with its multiparticle and vertex tracking capabilities, was able to achieve these tracking goals.

An important aspect of the STAR experiment was the ability to measure and trigger on events with large charged-particle multiplicities, total electromagnetic energy, high- p_T π^0 s, jet energies and single and multiple high- p_T particles (including

π^0 s). STAR measured two-particle correlations over a large acceptance at mid-rapidity with good momentum resolution and using Hanbury-Brown and Twiss (HBT) interferometry techniques [9] was able to determine the size and lifetime of the particle-emitting source. It was anticipated that measurements would also be made in pp collisions and a range of p-A and A-A collisions.

A key early result from STAR was the measurement of the spectra and integrated yield ratios of identified hadrons at mid-rapidity in central Au-Au collisions. See [10] for details. Fig. 4 shows these ratios along with a fit from the statistical model. The yields of multi-strange baryons Ξ and Ω were observed to be considerably enhanced in central Au-Au collisions compared to pp collisions at similar energies. The measured ratios constrain the values of the system temperature and the baryon chemical potential μ_B at chemical freeze-out T_{ch} . Furthermore, the strangeness saturation parameter γ_s increases with centrality as seen in the inset, where for the most central collisions $\gamma_s = 0.99 \pm 0.07$ compared to the much lower value for pp collisions, which is the leftmost point of the inset. The fits obtained from the ratios using the formulation of [11] are consistent with the assumption that the system is in thermal and chemical equilibrium at $T_{ch} = 163 \pm 5$ MeV.

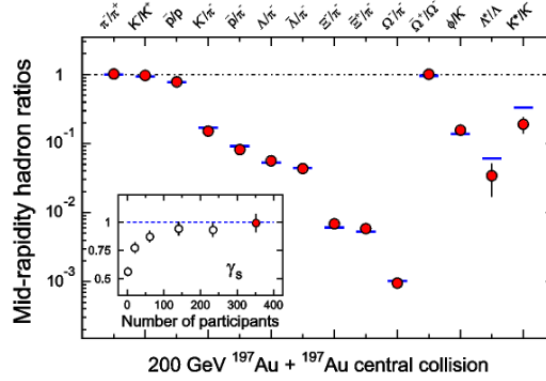


Fig. 4 Ratios of integrated mid-rapidity yields for various identified hadrons in central Au-Au collisions at $\sqrt{s_{NN}} = 200$ GeV measured in STAR [10]. Statistical model fits (horizontal bars) to the measured ratios give fit parameters $T_{ch} = 163 \pm 4$ MeV, $\mu_B = 24 \pm 4$ MeV, $\gamma_s = 0.99 \pm 0.07$. The variation of the strangeness saturation parameter γ_s with centrality is shown in the inset. See text.

A significant result from RHIC was the measurement of collective flow in Au-Au collisions [12]. The first indication that the hydrodynamic limit was reached at RHIC at the highest multiplicity densities can be seen in Fig. 5. The rightmost points represent the highest multiplicities in near-central collisions in STAR. There, the observed ratio of elliptic flow / shear viscosity (v_2/ϵ) is consistent with rapid thermalization (within ~ 1 fm / c) and reaches the limiting hydrodynamic expectations for an ideal relativistic fluid [10]. The hydrodynamic limits are represented by green horizontal bars drawn for each range of collision energies for a particular choice of equation

of state that assumes no phase transition in the system that is produced. See [13] for details. This means that the behavior of the system at RHIC can be described by hydrodynamics, whereas at the lower energies, the system does not reach the hydrodynamic limit.

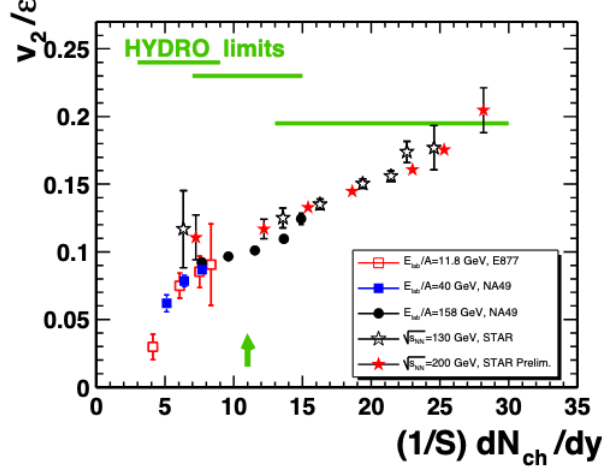


Fig. 5 Elliptic flow measurements at various energies and centralities showing v_2/ϵ (elliptic flow/initial spatial eccentricity) as a function of charged-particle rapidity density per unit transverse overlap area in the A-A collision. The v_2/ϵ rises smoothly versus energy and centrality. The highest energy STAR results [12] are consistent with limiting hydrodynamic expectations for an ideal relativistic fluid represented by green horizontal bars drawn for AGS, SPS and RHIC energies. From [13].

Once it was established that there was a highly-excited thermal medium, and collective flow at the highest energies in central A-A collisions, the experiments sought to find out whether high-momentum particles lose energy as they traverse the excited QGP medium. In order to compare with normal nuclear matter, an observable called the nuclear modification factor R_{AA} was measured and given by

$$R_{AA} = N_{AA} / \langle T_{AA} \rangle \times \sigma_{pp} \quad (1)$$

where N_{AA} is the number of observed particles per event of interest in A-A collisions, $\langle T_{AA} \rangle$ is the average value of the nuclear thickness function, and σ_{pp} is the particle production cross section in pp collisions at the same collision energy.

Fig. 6 (left panel) is the nuclear modification factor measured for Au-Au central collisions and d-Au collisions as a function of p_T [14]. The central Au-Au collisions exhibit a suppression of particles at high p_T compared to the d-Au collisions, indicating that the particles lose energy as they traverse the QGP medium formed in the central Au-Au collisions. Fig. 6 (right panel) shows angular correlations of particles at azimuthal angles $\Delta\phi$ relative to the peak ($\Delta\phi = 0$) in pp, d-Au, and Au-Au colli-

sions [15]. The peak represents the jet cone of particles around the high-momentum trigger particle. The peak of particles at 180° ($\Delta\phi = \pi$) away from the trigger particle in pp and d-Au collisions is due to binary scattering of incident particles. However, high-momentum particles in central Au-Au collisions have no peak at 180° ($\Delta\phi = \pi$) away from the trigger, which indicates quenching of the jet that traversed the highly excited QGP in the direction opposite the trigger.

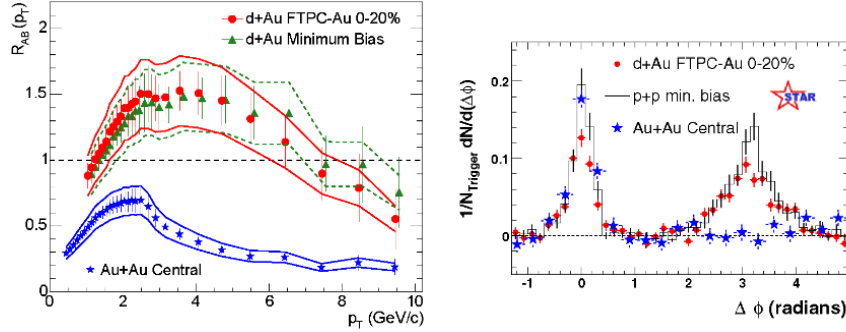


Fig. 6 (Left panel) R_{AA} for central Au-Au collisions and R_{AB} for the asymmetric d-Au collisions at $\sqrt{s_{NN}} = 200$ GeV as measured by STAR [14]. (Right panel) Dihadron azimuthal correlations at high p_T for p + p, central d + Au and central Au + Au collisions (with background subtracted) at $\sqrt{s_{NN}} = 200$ GeV from STAR [14, 15].

After the first years of RHIC operation and physics, STAR proposed various new detectors and upgrades that have since become an integral part of STAR and its physics. STAR added barrel and end-cap time-of-flight detectors, a compact muon detector, intermediate and forward tracking detectors, a forward meson spectrometer, an event-plane detector, a higher-rate data acquisition system, faster TPC readout and extended coverage of the TPC, and a forward silicon tracking and calorimeter upgrade.

These new detector upgrades enabled a broad expansion of the STAR heavy-ion physics program that has included interesting results on the suppression of quarkonia [16], thermal dileptons [17], ultra-peripheral collisions [18], an unexpected chiral magnetic effect [19], and new inquiry into how baryon charge is carried in these collisions [20]. Additional investigation has continued into the behavior of open heavy-flavor particles, higher-order flow harmonics and fluctuations, correlation lengths and susceptibilities of the QGP, jet quenching and substructure, and links to the nuclear equation of state via beam energy scans down below SPS energies.⁵ STAR has discovered new light antimatter nuclei and antimatter hypernuclei, for example $\bar{\Lambda}^4\bar{H}$; see [21] and the references therein for the achievements of the STAR antimatter nucleus program. In addition, recent observation by STAR of an unexpectedly large global spin alignment of the vector mesons (spin 1) ϕ and K^{*0} appears to only be

⁵ https://drupal.star.bnl.gov/STAR/files/BES_WP11_ver6.9_Cover.pdf

describable in terms of strong force fields in QCD. [22]. The detector performance and physics of the above studies continue to be presented at semiannual Quark Matter meetings.⁶

3 The PHENIX Experiment at RHIC

Immediately after the PHENIX collaboration was formed, the PHENIX goals and experiment were proposed in June 1992. The design proposed at that time is shown in Fig. 7. The US-Japan High Energy program sponsored by KEK held a review and decided to add $\geq \$10\text{M}$ to support the construction of a time-of-flight detector to measure hadrons, a ring imaging detector, and a transition radiation detector to measure e^+e^- pairs over a limited solid angle. In addition, an electromagnetic (EM) calorimeter was included to measure photons. A forward arm of PHENIX was planned for the measurement of $\mu^+\mu^-$ pairs, although resources were still needed to cover this portion.

In 1993, the RIKEN group proposed a polarized proton spin physics program at RHIC with Siberian snakes and spin rotators for both PHENIX and STAR. The RIKEN-Spin group joined PHENIX and the polarized proton program with one muon arm for PHENIX was approved by RIKEN in 1994. A second muon arm was approved by the US DOE in 1995, leading to the final configuration of PHENIX [23], which includes the two muon arms (RIKEN and DOE) shown in Fig. 7.

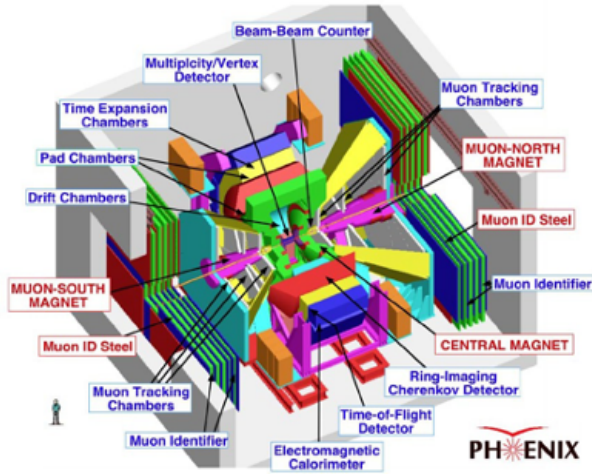


Fig. 7 The PHENIX Detector and subsystems as labeled. See [23] for reference and details.

⁶ See https://inspirehep.net/conferences?sort=dateasc&size=25&page=1&start_date=all&&q=QM

The initial physics goals of PHENIX were expected to be achieved in three steps, as illustrated in Fig. 8 [24]. First, PHENIX would measure the multiplicity up to the highest multiplicity, as seen in the top of the figure. Next, it would measure dE_T/dy with the EM calorimeters to determine R_T as illustrated in the middle of Fig. 8. Since the energy density ϵ can be given by

$$\epsilon = E/V = (dE_T/dy) / (\pi R_T^2 c \tau_0) \quad (2)$$

the third step was to measure as many potential signals as possible as a function of dE_T/dy (or equivalently as a function of ϵ).

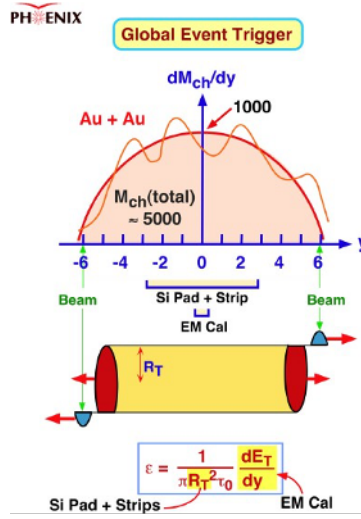


Fig. 8 PHENIX diagrams that illustrate its multiplicity measurement $M_{ch}(\text{top})$ that is used to deduce R_T (middle) with its calorimeter measurements of dE_T/dy and indicating (bottom) how they are used to determine the energy density ϵ . From [24].

It was predicted that the $c\bar{c}$ bound state would no longer exist at sufficiently high temperatures due to the Debye screening of QCD interactions between the c and \bar{c} quarks. Since J/ψ is a bound state of c and \bar{c} , J/ψ particle production would be strongly suppressed [25]. As the radius of ψ' is larger than J/ψ , the degree of suppression would be stronger for ψ' than for J/ψ . PHENIX planned to explore the systematic measurement of these vector mesons by detection of dielectrons and dimuons. In the 1990s, other predictions existed, such as measurements of QGP radiation, since the photon production mechanism differs considerably between a hadron gas and a quark-gluon gas [26]. Unfortunately, most of the predicted signals in the 1990s were not all easily accessible to experiment, justifying the experimental approach to measure multiple signals.

In the early running of RHIC, while PHENIX was accumulating the statistics necessary to be able to address the prediction of suppression of J/ψ , it also collected

data that significantly contributed to our understanding of jet quenching [27]. Fig. 9 shows the early charged-hadron and π^0 measurements from PHENIX in central Au-Au collisions at $\sqrt{s_{NN}} = 130$ GeV. The suppression observed in these measurements is compared with previous Pb-Pb measurements at CERN-SPS and $\alpha\alpha$ measurements at the CERN-ISR at $\sqrt{s_{NN}} = 17$ and 31 GeV, respectively. The lower energy measurements exhibit an enhancement that has been attributed to an anomalous nuclear enhancement, called the Cronin effect [28]. See [29] for more details.

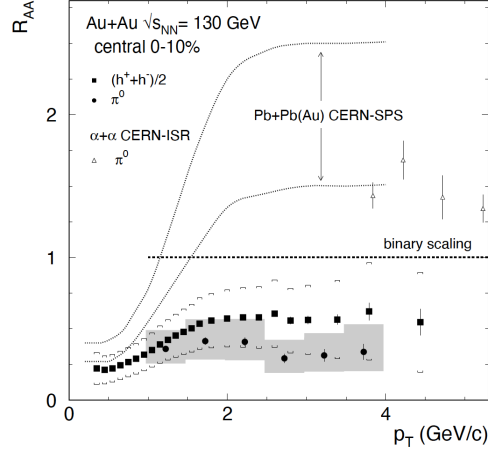


Fig. 9 Jet quenching measurements by PHENIX at the early RHIC energy of $\sqrt{s_{NN}} = 130$ GeV. Also shown are results from Pb-Pb measurements at the CERN-SPS ($\sqrt{s_{NN}} = 17$ GeV) and $\alpha\alpha$ measurements at the CERN-ISR ($\sqrt{s_{NN}} = 31$ GeV). From [29]. See text.

Shown in Fig. 10 are PHENIX R_{AA} measurements of identified π^0 , η and direct γ out to large values of p_T . The π^0 and η are suppressed, while the γ is not. Since γ does not interact via strong interactions, the fact that $R_{AA}(\gamma) \simeq 1$ provides strong evidence that the observed suppression of hadrons (π^0 and η) is due to their strong final-state interaction as they traverse the QGP.

PHENIX also collected important results on the elliptic flow that STAR observed. The PHENIX and STAR elliptic flow v_2 for identified particles are presented in Fig. 11 as a function of a) particle p_T and b) particle transverse kinetic energy KE_T , where $KE_T = m_T - m$, taken from [30]. The data in the left panels appear to separate into two curves, one for the mesons and the other for baryons. When the elliptic flow is divided by the number of quarks (n_q) in each particle ($n_q = 2$ for mesons and 3 for baryons), and v_2/n_q is plotted as a function of the transverse kinetic energy per quark KE_T/n_q all particles fall on the same curve as seen in the panel on the right. This constituent quark number scaling establishes that the collective flow developed in the quark stage, rather than a later hadronic stage.

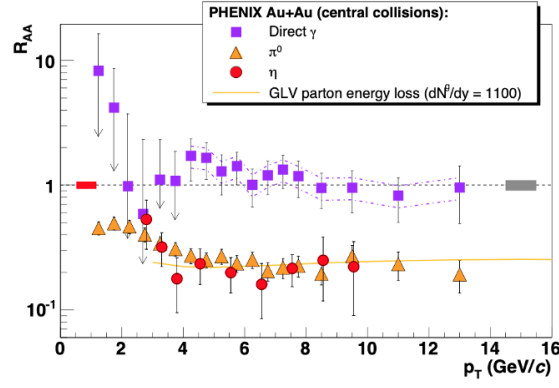


Fig. 10 R_{AA} measured by PHENIX for π^0 , η , and direct γ as a function of p_T in central $\sqrt{s_{NN}} = 200$ GeV Au-Au collisions. See text and [29] for details.

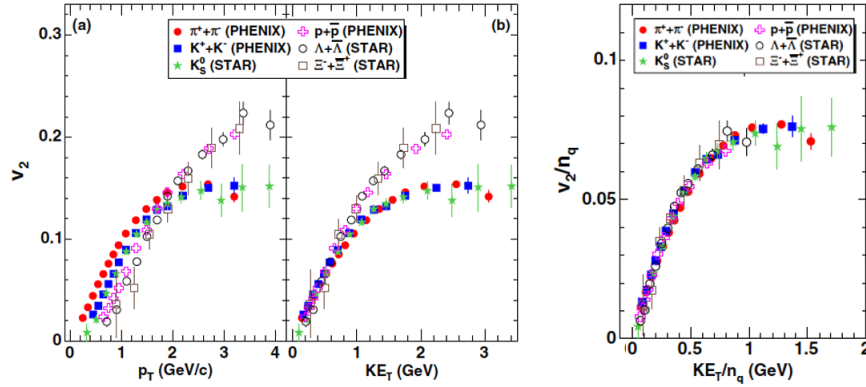


Fig. 11 Left double panel: a) Elliptic flow (v_2) for particles identified in the inset by PHENIX and STAR versus particle p_T . b) Elliptic flow versus particle transverse kinetic energy KE_T . Right panel: Elliptic flow per quark v_2/n_q versus the transverse kinetic energy per quark KE_T/n_q , revealing that constituent quark number scaling holds, which is observed by all particles falling on the same curve. From [30].

After the first few years of RHIC running, PHENIX was able to collect sufficient statistics for its J/ψ , heavy-flavor, and photon programs. It observed a suppression of $R_{AA}(J/\psi)$ [31], and suppression of nonphotonic electron spectra due to semileptonic decays of heavy-quark hadrons [32], while direct-photon yields were observed to scale with the number of nucleon-nucleon collisions. These results further confirmed that the large suppression of high p_T hadrons is a final-state effect due to parton energy loss in the QGP [33]. Among subsequent publications, PHENIX studied collisions in three small systems with very different intrinsic initial geometries and found that

the hydrodynamic model with a QGP was able to describe the three systems [34], confirming the influence of the initial-state effects on azimuthal correlations.

PHENIX ended its data collection campaign in 2015 and began preparations for its successor, a new fast state-of-the-art detector called sPHENIX. The purpose of sPHENIX is to investigate and understand the microscopic structure of the QGP and to reveal how strongly interacting matter can arise from the interactions of quarks and gluons described by QCD. A description of sPHENIX and predictions for the breadth of its physics program can be found in [35]. sPHENIX started collecting data at RHIC in 2023.

With the support of RIKEN, the RHIC spin program has sought to measure the origin of the spin of the proton, which offered additional compelling physics measurements at RHIC for PHENIX and STAR. The data on deep-inelastic lepton scattering by nucleons indicated that quarks carry only about 30% of the spin of the nucleon [36]. The remaining $\sim 70\%$ must then come from other mechanisms such as gluon polarization, antiquark polarization, or orbital angular momentum inside the nucleus, as schematically illustrated in Fig. 12.

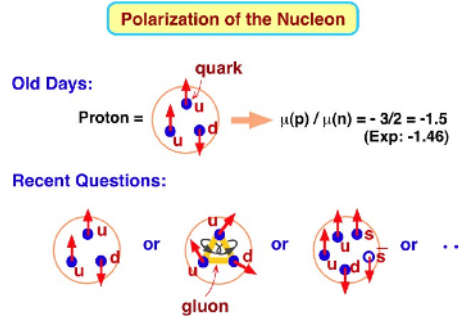


Fig. 12 The purpose of studies using polarized protons is to understand the origin of the nucleon spin, since only 30% appears to be carried by quarks. From [24].

Experimentally, the asymmetry between polarized protons is measured in such configurations: $p(\rightarrow)$ vs. $p(\leftarrow)$ or $p(\uparrow)$ vs. $p(\downarrow)$. For example, if the gluon carries the nucleon spin, then measurements of the asymmetry of the following channels are of interest: $\text{gluon} + \text{gluon} \rightarrow \text{jet} + \text{jet}$, and $\text{gluon} + q \rightarrow \text{high-energy } \gamma + \pi^0$. On the other hand, if anti-quarks carry the nucleon spin, the channels of interest are: $q + \bar{q} \rightarrow W \rightarrow e \text{ (or } \mu) + \nu$ (as in beta-decay).

Once the asymmetry parameters are measured in polarized-proton collisions, the results can be quantitatively connected to the individual components of the spin inside the nucleon. In particular, the PHENIX EM calorimeter was able to measure high-energy photons and e and μ , while STAR measures jet-jet correlations to determine these asymmetry parameters and the various contributions to the spin of the proton. These studies are ongoing at RHIC.

4 The PHOBOS Experiment at RHIC

After evaluation of the initial proposed experiments, as mentioned earlier, RHIC management decided that there would be two large detectors and two small detectors. In response, a group of physicists from Argonne National Lab, Brookhaven National Lab, INP Krakow Poland, the Massachusetts Institute of Technology, National Central University Chung-Li Taiwan, the University of Illinois at Chicago, the University of Maryland, and the University of Rochester proposed the PHOBOS⁷ experiment, as one of the two small detectors. The design was based on the realization that: first, we did not know what would be the most interesting physics; second, shortly after RHIC the much higher energy LHC would begin operations; third, a small group must limit the number of technologies it has to develop; and last and most important, that after the initial studies at RHIC, the small detectors would not be competitive with the two bigger, more expensive ones.

These considerations led to the following strategy. Build a detector with which one can look at the first physics, particularly the global features, learn as much as possible, and then move to heavy ions at the LHC, using as a guide the results obtained at RHIC. Looking back, it is remarkable how well this strategy worked. In essence, a single technology was used (silicon detectors, with all sensors constructed by one manufacturer in Taiwan and all support structures manufactured from carbon fiber by one group in Poland), and thus crucial parts of PHOBOS were ready at the start of RHIC, so that the experiment obtained publishable results from RHIC within hours of the first collisions [37]. It also mapped out the global features of heavy-ion collisions at RHIC energies, and, finally, after the first round of RHIC experiments was completed, many of the members of PHOBOS moved on to continue their studies at the LHC.

Fig. 13 is a sketch of the PHOBOS detector [38]. Basically, it consists of two systems. One is an array of silicon detectors (labeled Octagon, Vertex and Ring), which detects charged particles produced in almost the entire solid angle around the collision point. Its design was inspired by an analogous experiment studying particle production in p-A collisions carried out in the 1970s at Fermilab [39]. The other system is a small acceptance magnetic spectrometer looking at low-momentum identified particles produced at mid-rapidity, the region where the highest energy density was expected to be produced.

The idea was that the pseudo-rapidity and azimuthal distributions of all the produced particles would give a global picture of particle production at RHIC, including the energy density produced and the extent to which A-A collisions differ from a superposition of independent pp interactions. On the other hand, the spectrometer was focused on a search for an anomalous production of very low-momentum particles,

⁷ In an earlier round of reviews, the same collaboration proposed a detector called MARS, an acronym for "Modular Array for RHIC Spectrometer". It was not accepted because of its scope and cost. Theorist John Negele suggested that, when a smaller, less expensive detector was proposed, it should be called PHOBOS, the larger moon of MARS. In this way, if the PHOBOS proposal was still too expensive and an even smaller, less expensive, one had to be built, a name would already be ready for it; DEIMOS, the smaller of the Martian moons!

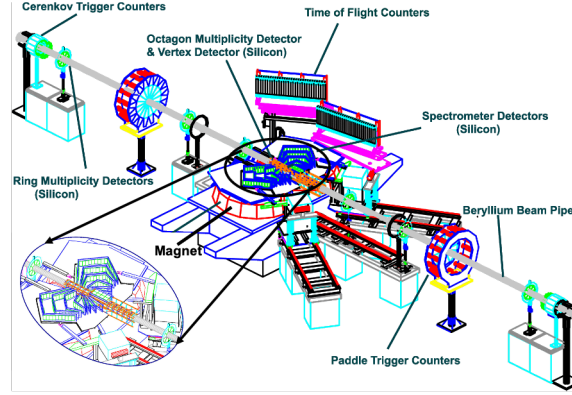


Fig. 13 The PHOBOS Detector Layout. See text and [38] for reference and details.

which would be a sign that a large volume of weakly interacting constituents had been produced. The results from PHOBOS can be found in [40].

Examples of pseudo-rapidity distributions measured by PHOBOS [41] are shown in Fig. 14. The event-by-event knowledge of the density of produced particles in all directions (i.e. both in rapidity and azimuth) encodes the complete particle production process, from the instant of collision, through the evolution of the intermediate state, including the production and decay of a possible QGP, to the hadronization of the finally produced hadrons. Thus, detailed knowledge of such data is crucial for a full understanding of the physics at play in heavy-ion collisions. In the PHOBOS multiplicity array, for example, the measured azimuthal distributions [42] showed, together with the other experiments, that there was a liquid intermediate state and that the produced liquid was a strongly interacting fluid with extremely low viscosity-to-entropy ratio, as opposed to the expected weakly interacting one. The measured particle density at mid-rapidity gave information on the dependence on energy and incident system of the maximum energy density released in the collisions.

Fig. 15 compares the particle density measured by PHOBOS with lower energy data and various theoretical model predictions [43] made before the onset of RHIC. As can be seen, most models over-predicted the mid-rapidity particle density, and therefore also the produced energy density. However, even the lower values found in the data showed that an energy density high enough to be interesting was being produced, which was a great relief for the community. Other results obtained with the multiplicity array were the discovery of participant scaling of the total particle multiplicity produced in heavy-ion collisions and the observation of extended longitudinal scaling [40], which is the extension in rapidity of the phenomenon known as limited fragmentation [44] and is direct evidence of saturation effects. Finally, an interesting observation was the fact that overall the data appear to be simpler than the theoretical explanations! For example, the centrality and energy dependences of several observables were found to factorize to a surprising degree [41]. Also, no significant discontinuities of any kind as a function of any variable were seen, early

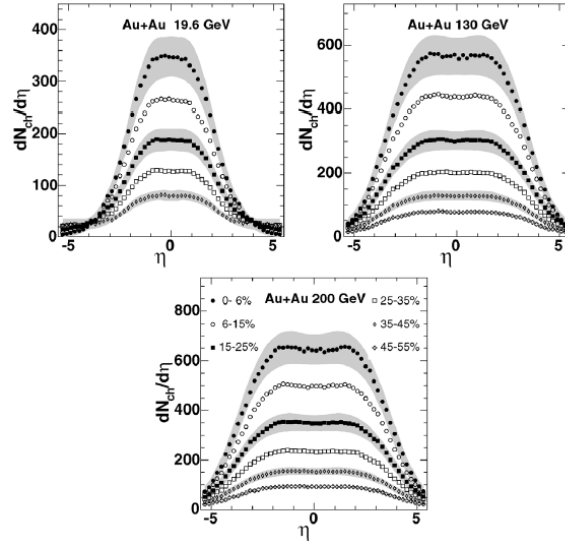


Fig. 14 Pseudo-rapidity density of charged particles emitted in Au-Au collisions at three different values of the nucleon–nucleon center-of-mass energy as measured by PHOBOS. Shown are data for bins of centrality as labeled in the bottom panel, binned by the fraction of the total inelastic cross section in each bin. The systematic uncertainties are represented as the gray bands (at the 90% confidence level). Statistical errors are smaller than the symbols. From [40].

signs that if there is a phase transition, it is more likely to be a cross-over rather than a first-order transition.

The suppression of high transverse momentum particles, called “jet quenching”, was observed using the spectrometer [45]. These observations were consistent with measurements made by the other experiments. A unique result obtained with the PHOBOS spectrometer was the observation that there is no evidence of an enhancement of low- p_T particles [40, 46], which would be indicative of the presence of unusual long-wave phenomena and an early sign that the medium produced is strongly interacting, a very important conclusion that was not fully appreciated at the time. The observed flattening of the spectra with p_T increases with the mass of the particle as seen in Fig. 16, supporting an interpretation of the data in terms of collective transverse expansion, and is naturally accounted for in the description of the evolution of the system based on hydrodynamic calculations [47].

Although the PHOBOS collaboration, in preparation for the LHC and sPHENIX experiments, ceased to take data after 2005, analysis of the data already collected continued for a number of years. During this period, PHOBOS developed the concept of participant eccentricity and carried out pioneering studies of the long-range nature of the “ridge” phenomenon. The former elucidated the importance of the geometric distribution of the nucleons in the nuclei at the instant of collision [48]. The latter is evidence of the importance of long-range rapidity correlations of the produced

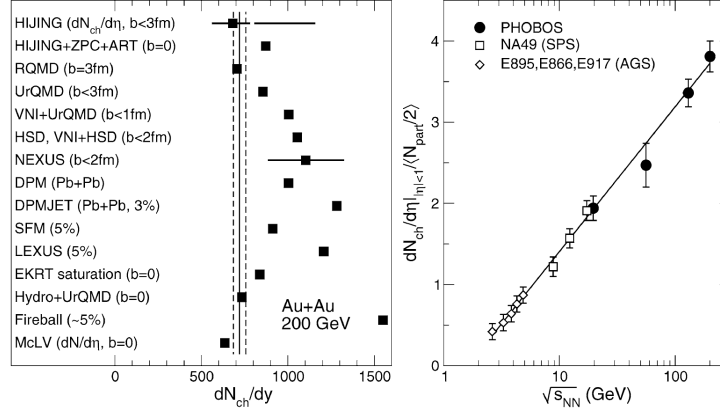


Fig. 15 Results from PHOBOS on the charged-particle density near mid-rapidity in Au-Au collisions at $\sqrt{s_{NN}} = 200$ GeV (represented by the vertical line, with the dashed lines denoting the systematic uncertainties), compared with lower energy data and theoretical predictions [43]. For details see [40].

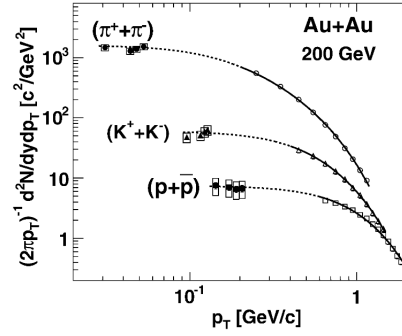


Fig. 16 Yields of identified charged particles measured by PHOBOS at very low p_T , compared with extrapolations of PHENIX measurements at intermediate p_T . Figure is from [40]. For discussion see text.

particles [49]. This eventually led to a unified view of the connection between initial-state fluctuations and final-state correlations in terms of triangularity, triangular flow, and other higher-order components.

4.1 The BRAHMS Experiment at RHIC

The smallest of the RHIC experiments was BRAHMS (Broad Range Magnetic Spectrometer) with 40 members and 11 institutions. It was inspired by the CERN ISR experience; at the time when the ISR experiments were in the planning stage, the most interesting questions were thought to be particle production in the forward and backward directions. Thus, the focus of the ISR detectors was on particles produced in those directions. Right from the start of data taking it became clear that the reality is exactly the opposite and the detectors had to be reconfigured to study particles produced at mid-rapidity! At the time of planning the first round of RHIC experiments, the conventional wisdom was that the most interesting physics will be learned from studies of particles produced at mid-rapidity, those from the hottest region of the produced state. Thus, the PHENIX, PHOBOS, and STAR collaborations all decided to concentrate on the study of these particles. In order that the ISR mistake would not be repeated at RHIC, the BRAHMS collaboration decided to construct a detector where its greatest asset was its acceptance in the forward and backward directions, where the other detectors are weakest.

A sketch of the BRAHMS detector is shown in Fig. 17 with details described in [50]. It consists of two magnetic spectrometers with excellent momentum resolution and hadron identification capability. Each subtends a small solid angle but can rotate about the collision point and thus can obtain inclusive data for hadron production over a wide range of rapidity.

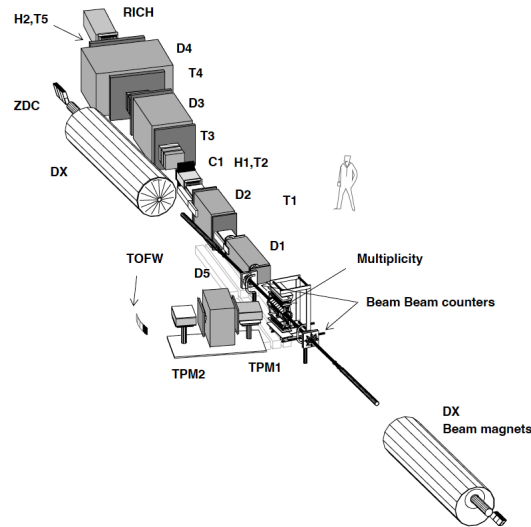


Fig. 17 BRAHMS detector layout. See [50] for reference and details.

With this detector BRAHMS could study, as a function of centrality, identified spectra of p , K , and π in the range $0 \leq y \leq 4$ and $0.2 \leq p_T \leq 3$ GeV/c. It should be emphasized that BRAHMS was the only RHIC experiment that could measure, over this large kinematic range, the true rapidity and not just the pseudo-rapidity. The aim was to address questions such as what is the energy available for particle production, what is the longitudinal extent of the near baryon-free medium, what is the medium created at mid-rapidity, how does the "chemistry" of the medium change with rapidity, are small- x effects (saturation) evident in the forward direction. The results from BRAHMS can be found in [51]. An example of BRAHMS results is given in Fig. 18, where the measured rapidity density of net protons for central collisions is shown, compared to lower-energy data. From these data it was concluded that at RHIC energies the rapidity loss of the incident protons is approximately 2 units, consistent with expectations from extrapolations of p-A data obtained at Fermilab in the early 1980s.

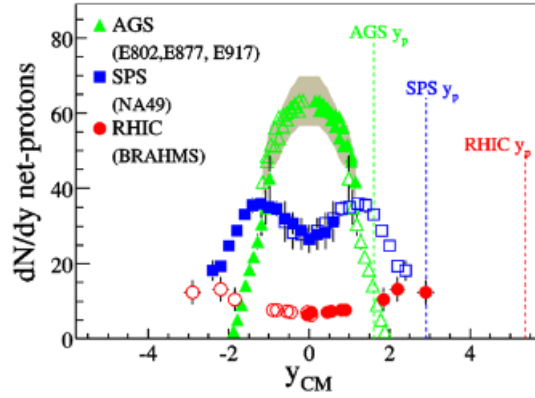


Fig. 18 Rapidity density of net protons (number of protons minus number of antiprotons) measured at AGS, SPS, and RHIC for central collisions, from BRAHMS [51]. BRAHMS was able to extend its unique high-statistics measurements to $y = 3.5$ in $\sqrt{s_{NN}} = 200$ GeV Au-Au, corresponding to measurements to within 2.3 degrees of the beam direction.

5 Pre-RHIC to Post-RHIC

As discussed earlier, in the late 1970s and early 1980s it was thought that in experimentally accessible heavy-ion collisions it should be possible to produce energy densities above 1 GeV/fm^3 , and it was expected that at such densities a very interesting phase of QCD should exist: a QCD gas of weakly interacting, free quarks and gluons named the QGP. Furthermore, that there is a first-order transition between a

hadron gas and the QGP and therefore it should be easy to discover and study. Fig. 19 illustrates examples of “results” that, with luck, would be observed and that would be clear evidence of a phase transition taking place [52].

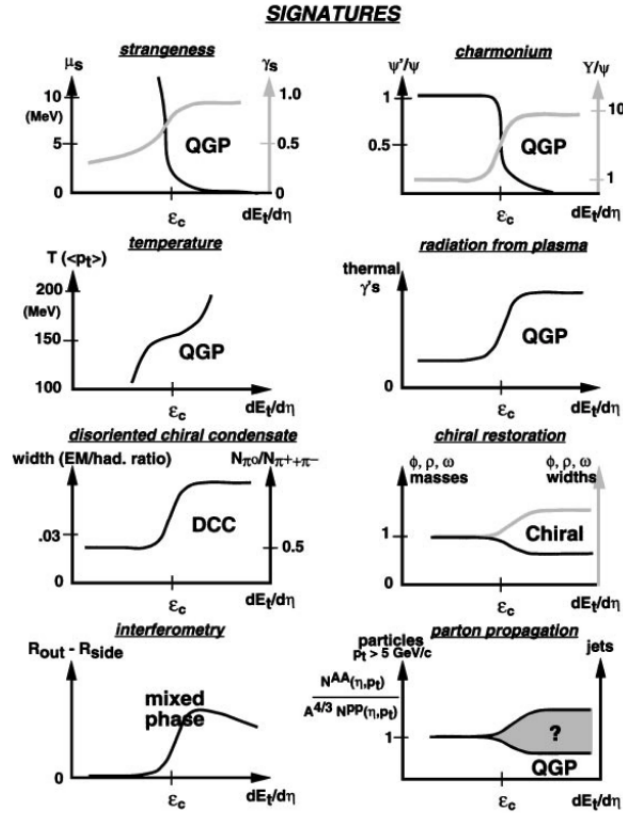


Fig. 19 Behavior of some of the potential QGP signatures anticipated in 1996, prior to RHIC. From Ref.[52]

It was this kind of thinking that gave rise to the decision to build RHIC and, while waiting, to convert existing proton accelerators to produce as high an energy ion accelerator as possible and use them to collide the beams with stationary nuclei to begin a search for evidence of QGP production.

Reality proved not to be so simple! As discussed in the section of this book describing studies using the AGS accelerator at Brookhaven and the SPS at CERN there were many tantalizing results, but no sign of discontinuities that would show a first-order phase transition, in any variable studied.

By the year 2000, when RHIC became operational and gold nuclei were collided, first at a center of mass energy of 56 GeV/nucleon, and then up to 200 GeV/nucleon,

the community was divided on their opinion whether there is or is not any evidence for the creation of the QGP at the AGS or SPS energies.

From the first collisions, the RHIC results were a bomb-shell and a game changer! There was no evidence of any discontinuities of observed quantities, which would be indicative of a first-order phase transition, and no signs of any weakly-interacting quark-gluon gas. In contrast, the RHIC experiments, to a lesser or greater extent, found that, rather than a weakly-interacting gas being produced, there is strong evidence for the creation of a very strongly-interacting liquid; a liquid with a remarkably low ratio of shear viscosity to entropy. This conclusion followed primarily from two observations; first, the azimuthal angular distributions of the produced particles could be explained by assuming that they obeyed the equations of relativistic hydrodynamics and second, as can be seen in Fig. 20, that high-energy particles lose a significant fraction of their energy as they traverse the medium produced in the collision, a phenomenon called jet quenching. At the time this was considered so important that the jet quenching data, from all four RHIC experiments, appeared on the cover of *Physical Review Letters* (Fig. 20)! An important workshop was held at the end of the first round of experiments in May 2004 to discuss the state of knowledge of hot QCD. The proceedings of the workshop [54] and its accompanying "white papers" [55] summarize the results from the four RHIC experiments and provide an excellent overview of the field of relativistic heavy-ion collisions at the beginning of the 21st century.

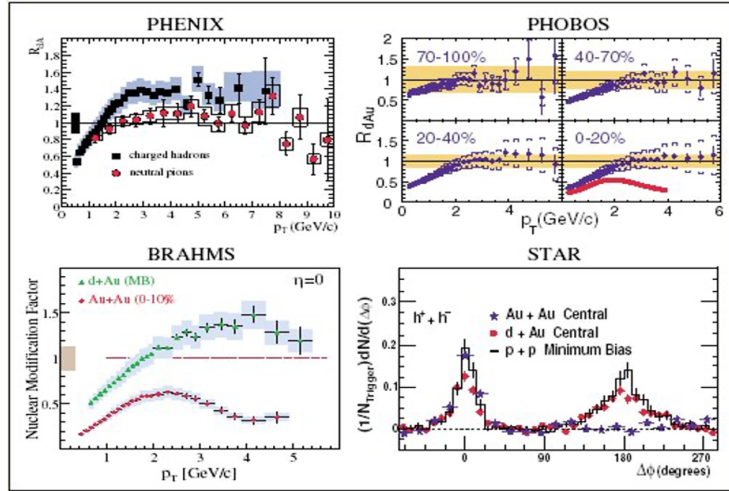


Fig. 20 Nuclear modification factor in $\sqrt{s_{NN}} = 200$ GeV d-Au relative to that from pp collisions for: (upper left) PHENIX inclusive charged hadrons and π^0 s, and (upper right) PHOBOS charged particles for four d-Au centrality bins and in red symbols central (0–6%) Au-Au data. (lower left) BRAHMS charged particles in minimum bias d-Au and central Au-Au at $\sqrt{s_{NN}} = 200$ GeV. (lower right) STAR angular correlation of charged hadrons in Au-Au, d-Au and pp as labeled. This figure indicates jet quenching in Au-Au but not in d-Au and disappearance of the away-side jet in central Au-Au. Figure from the cover of *Physical Review Letters* [53].

In retrospect, we have a fairly good understanding of what went wrong with the prediction that the QGP is a weakly interacting gas. There was an erroneous interpretation of some lattice QCD simulations, unrealistic assumptions about how fast the running of the strong coupling constant would lead to a weakly interacting gas, and not understanding well the application of the non-perturbative QCD regime to heavy-ion collisions. Most importantly, we now know that the transition from a hadron gas to the QGP is not a phase transition. It is a cross-over and this explains the smooth behavior of all measurements.

In reality, the fact that a first-order phase transition to a weakly-interacting QGP was not discovered and does not exist is fortuitous! If a non-interacting gas was discovered at RHIC, it would have killed the field. There would be nothing to study!

As it is, RHIC opened a fascinating and rich field of studies that now continues at the LHC. We still do not thoroughly understand the properties of the QGP, the phenomenon of jet quenching, the physics that takes place in multiparticle production from the instant of collision to the final production of outgoing hadrons, and most importantly, how a complex form of matter, such as the QGP, emerges from simple underlying laws and particles.

References

1. N. P. Samios, "RHIC: The early years," *J. Phys. G* **34**, S181-S189 (2007).
2. T. W. Ludlam and H. E. Wegner, "REPORT OF THE ROUND TABLE DISCUSSION OF PROSPECTS FOR FUTURE EXPERIMENTS," *Nucl. Phys. A* **418**, 375C-377C (1984).
3. R. Hagedorn, "Statistical thermodynamics of strong interactions at high-energies," *Nuovo Cim. Suppl.* **3**, 147-186 (1965) CERN-TH-520; J. Rafelski and T. Ericson: "The tale of the Hagedorn temperature," *CERN Cour.* **43N7**, 30-33 (2003).
4. W. Busza and A.S. Goldhaber, "Nuclear stopping power", *Physics Letters B* **139** (1984) 235.
5. S. Nagamiya, "Toward New Forms of Nuclear Matter With Relativistic Heavy Ion Collisions," *Nucl. Phys. A* **488**, 3C-30C (1988).
6. "The Relativistic Heavy Ion Collider Project: RHIC and its Detectors," *Nuclear Instruments and Methods in Physics Research A* **499** (2003) v-xii.
7. K.H. Ackermann et al. [STAR], "STAR detector overview," *Nuclear Instruments and Methods in Physics Research A* **499** (2003) 624-632 and references therein.
8. B. Muller, "Hadronic Matter in Collisions 1988," *World Scientific* (1989), editors P. Carruthers and J. Rafelski, p. 379 and references therein.
9. M. Gyulassy, S. K. Kauffmann and L. W. Wilson, "Pion Interferometry of Nuclear Collisions. 1. Theory," *Phys. Rev. C* **20**, 2267 (1979).
10. J. Adams *et al.* [STAR], "Experimental and theoretical challenges in the search for the quark gluon plasma: The STAR Collaboration's critical assessment of the evidence from RHIC

- collisions,” Nucl. Phys. A **757**, 102-183 (2005).
11. P. Braun-Munzinger, I. Heppe and J. Stachel, “Chemical equilibration in Pb + Pb collisions at the SPS,” Phys. Lett. B **465**, 15-20 (1999).
 12. K. H. Ackermann *et al.* [STAR], “Elliptic flow in Au + Au collisions at $\sqrt{s_{NN}} = 130$ GeV,” Phys. Rev. Lett. **86**, 402-407 (2001).
 13. C. Alt *et al.* [NA49], “Directed and elliptic flow of charged pions and protons in Pb + Pb collisions at 40-A-GeV and 158-A-GeV,” Phys. Rev. C **68**, 034903 (2003).
 14. J. Adams *et al.* [STAR], “Evidence from d + Au measurements for final state suppression of high p_T hadrons in Au+Au collisions at RHIC,” Phys. Rev. Lett. **91**, 072304 (2003).
 15. C. Adler *et al.* [STAR], “Disappearance of back-to-back high p_T hadron correlations in central Au+Au collisions at $\sqrt{s_{NN}} = 200$ -GeV,” Phys. Rev. Lett. **90**, 082302 (2003).
 16. B. Aboona *et al.* [STAR], “Observation of sequential Υ suppression in Au+Au collisions at $\sqrt{s_{NN}} = 200$ GeV with the STAR experiment,” Phys. Rev. Lett. **130**, no.11, 112301 (2023), see references therein.
 17. M. I. Abdulhamid *et al.* [STAR], “Measurements of dielectron production in Au+Au collisions at $\sqrt{s_{NN}} = 27, 39$, and 62.4 GeV from the STAR experiment,” Phys. Rev. C **107**, no.6, L061901 (2023), see references therein.
 18. M. I. Abdulhamid *et al.* [STAR], “Observation of Strong Nuclear Suppression in Exclusive J/ψ Photoproduction in Au+Au Ultraperipheral Collisions at RHIC,” Phys. Rev. Lett. **133**, no.5, 052301 (2024), see references therein.
 19. M. I. Abdulhamid *et al.* [STAR], “Upper limit on the chiral magnetic effect in isobar collisions at the Relativistic Heavy-Ion Collider,” Phys. Rev. Res. **6**, no.3, L032005 (2024), see references therein.
 20. The STAR Collaboration, “Tracking the baryon number with nuclear collisions,” [arXiv:2408.15441 [nucl-ex]], see references therein.
 21. M. Abdulhamid *et al.* [STAR], “Observation of the antimatter hypernucleus $_{\Lambda}^4\bar{\text{H}}$,” Nature **632**, no.8027, 1026-1031 (2024).
 22. M. S. Abdallah *et al.* [STAR], “Pattern of global spin alignment of ϕ and K^{*0} mesons in heavy-ion collisions,” Nature **614**, no.7947, 244-248 (2023).
 23. K. Adcox *et al.* [PHENIX], “PHENIX detector overview,” Nuclear Instruments and Methods in Physics Research A **499** (2003) 469–479 and references therein.
 24. S. Nagamiya, “Scientific endeavors towards RHIC and the PHENIX experiment,” PTEP **2015**, no.3, 03A101 (2015).
 25. T. Matsui and H. Satz, “ J/ψ suppression by quark-gluon plasma formation”, Phys. Lett. B **178**, 416 (1986).
 26. P. V. Ruuskanen, “Electromagnetic probes of quark-gluon plasma in relativistic heavy ion collisions”, Nucl. Phys. A **544**, 169 (1992).

27. K. Adcox *et al.* [PHENIX], “Formation of dense partonic matter in relativistic nucleus-nucleus collisions at RHIC: Experimental evaluation by the PHENIX collaboration,” Nucl. Phys. A **757**, 184-283 (2005)
28. D. Antreasyan, J. W. Cronin, H. J. Frisch, M. J. Shochet, L. Kluberg, P. A. Piroue and R. L. Sumner, “Production of Hadrons at Large Transverse Momentum in 200-GeV, 300-GeV and 400-GeV p p and p n Collisions,” Phys. Rev. D **19**, 764-778 (1979).
29. K. Adcox *et al.* [PHENIX], “Suppression of hadrons with large transverse momentum in central Au+Au collisions at $\sqrt{s_{NN}} = 130$ -GeV,” Phys. Rev. Lett. **88**, 022301 (2002); T. C. Awes [PHENIX], “Highlights from PHENIX - II,” J. Phys. G **35**, 104007 (2008).
30. A. Adare *et al.* [PHENIX], “Scaling properties of azimuthal anisotropy in Au+Au and Cu+Cu collisions at $\sqrt{s_{NN}} = 200$ GeV,” Phys. Rev. Lett. **98**, 162301 (2007).
31. A. Adare *et al.* [PHENIX], “ J/ψ Production vs Centrality, Transverse Momentum, and Rapidity in Au+Au Collisions at $\sqrt{s_{NN}} = 200$ GeV,” Phys. Rev. Lett. **98**, 232301 (2007).
32. S. S. Adler *et al.* [PHENIX], “Nuclear modification of electron spectra and implications for heavy quark energy loss in Au+Au collisions at $\sqrt{s_{NN}} = 200$ GeV,” Phys. Rev. Lett. **96**, 032301 (2006).
33. S. Afanasiev *et al.* [PHENIX], “Measurement of Direct Photons in Au+Au Collisions at $\sqrt{s_{NN}} = 200$ GeV,” Phys. Rev. Lett. **109**, 152302 (2012).
34. C. Aidala *et al.* [PHENIX], “Creation of quark–gluon plasma droplets with three distinct geometries,” Nature Phys. **15**, no.3, 214-220 (2019).
35. R. Belmont, J. Brewer, Q. Brodsky, P. Caucal, M. Connors, M. Djordjevic, R. Ehlers, M. A. Escobedo, E. G. Ferreira and G. Giacalone, *et al.* “Predictions for the sPHENIX physics program,” Nucl. Phys. A **1043**, 122821 (2024).
36. R. L. Jaffe and A. Manohar, “The g1 problem: Deep inelastic electron scattering and the spin of the proton”, Nucl. Phys. B337, 509 (1990).
37. B. B. Back *et al.* [PHOBOS], “Charged particle multiplicity near mid-rapidity in central Au + Au collisions at $\sqrt{s_{NN}} = 56$ GeV and 130 GeV,” Phys. Rev. Lett. **85**, 3100-3104 (2000).
38. B.B. Back *et al.* [PHOBOS], “The PHOBOS detector at RHIC,” Nuclear Instruments and Methods in Physics Research A 499 (2003) 603–623 and references therein.
39. J. E. Elias, W. Busza, C. Halliwell, D. Luckey, P. Swartz, L. Votta and C. Young, “An Experimental Study of Multiparticle Production in Hadron - Nucleus Interactions at High Energy,” Phys. Rev. D **22**, 13 (1980).
40. B. B. Back *et al.* [PHOBOS], “The PHOBOS perspective on discoveries at RHIC,” Nucl. Phys. A **757**, 28-101 (2005)
41. B. Alver *et al.* [PHOBOS], “PHOBOS results on charged particle multiplicity and pseudorapidity distributions in Au+Au, Cu+Cu, d+Au, and p+p collisions at ultra-relativistic energies,” Phys. Rev. C **83**, 024913 (2011).
42. B. B. Back *et al.* [PHOBOS], “Centrality and pseudorapidity dependence of elliptic flow for charged hadrons in Au+Au collisions at $\sqrt{s_{NN}} = 200$ GeV,” Phys. Rev. C **72**, 051901 (2005).

43. K. J. Eskola, “On predictions of the first results from RHIC,” Nucl. Phys. A **698**, 78-87 (2002).
44. J. Benecke, T. T. Chou, C. N. Yang and E. Yen, “Hypothesis of Limiting Fragmentation in High-Energy Collisions,” Phys. Rev. **188**, 2159-2169 (1969).
45. B. Alver *et al.* [PHOBOS], “System size and centrality dependence of charged hadron transverse momentum spectra in Au + Au and Cu + Cu collisions at $\sqrt{s_{NN}} = 62.4$ GeV and 200 GeV,” Phys. Rev. Lett. **96**, 212301 (2006).
46. B. B. Back *et al.* [PHOBOS], “Identified hadron transverse momentum spectra in Au+Au collisions at $\sqrt{s_{NN}} = 62.4$ GeV,” Phys. Rev. C **75**, 024910 (2007).
47. P. F. Kolb and R. Rapp, “Transverse flow and hadrochemistry in Au+Au collisions at $\sqrt{s_{NN}} = 200$ GeV,” Phys. Rev. C **67**, 044903 (2003).
48. B. Alver *et al.* [PHOBOS], “Non-flow correlations and elliptic flow fluctuations in gold-gold collisions at $\sqrt{s_{NN}} = 200$ GeV,” Phys. Rev. C **81**, 034915 (2010).
49. B. Alver *et al.* [PHOBOS], “High transverse momentum triggered correlations over a large pseudorapidity acceptance in Au+Au collisions at $\sqrt{s_{NN}} = 200$ GeV,” Phys. Rev. Lett. **104**, 062301 (2010).
50. M. Adamczyk *et al.* [BRAHMS], “The BRAHMS experiment at RHIC,” Nuclear Instruments and Methods in Physics Research A 499 (2003) 437–468 and references therein.
51. I. Arsene *et al.* [BRAHMS], “Quark gluon plasma and color glass condensate at RHIC? The Perspective from the BRAHMS experiment,” Nucl. Phys. A **757**, 1-27 (2005)
52. J. W. Harris and B. Müller, “The Search for the quark-gluon plasma,” Ann. Rev. Nucl. Part. Sci. **46**, 71 (1996); and ““QGP Signatures Revisited”,” Eur. Phys. J. C **84**, no.3, 247 (2024).
53. Physical Review Letters 91 (7), 070401– 079702, 15 August 2003.
54. D. Rischke and G. Levin, “Quark gluon plasma. New discoveries at RHIC: A case of strongly interacting quark gluon plasma. Proceedings, RBRC Workshop, Brookhaven, Upton, USA, May 14-15, 2004,” Nucl. Phys. A **750**, pp.1-169 (2005).
55. “First Three Years of Operation of RHIC” Nucl. Phys. A **757**, 1-284 (2005).